Article

Probabilistic Analysis of an RL Circuit Transient Response under Inductor Failure Conditions

Muhammad Farooq-i-Azam [1], Zeashan Hameed Khan [2], Syed Raheel Hassan [3] and Rameez Asif [3,*]

1 Department of Electrical and Computer Engineering, COMSATS University Islamabad, Lahore Campus, Lahore 54600, Pakistan
2 Department of Avionics Engineering, College of Aeronautical Engineering, National University of Sciences & Technology, Islamabad 44000, Pakistan
3 School of Computing Sciences, University of East Anglia, Norwich NR4 7TJ, UK
* Correspondence: rameez.asif@uea.ac.uk

Abstract: We apply probability theory for the analysis of the exponentially decaying transient response of a resistor inductor electric circuit with partially known value of the inductance due to its failure. The inductance is known to be within a continuous interval, and the exact value is unknown, which may happen as a result of inductor faults due to a variety of factors—for example, when the circuit is deployed in an unusually harsh environment. We consider the inductance as a continuous uniform random variable for our analysis, and the transient voltage is treated as a derived random variable which is a function of the inductance random variable. Using this approach, a probability model of the transient voltage at the output terminals of the circuit is derived in terms of its cumulative distribution function and the probability density function. In our work, we further elaborate that the probability model of any other circuit parameter can also be obtained in a similar manner, or it can be derived from the transient voltage probability model. This is demonstrated by getting the model of a branch current from the probability distribution of the transient voltage. Usage of the probability model is demonstrated with the help of examples. The probability of the transient voltage falling in a certain interval at a given instant of time is evaluated. Similarly, the probability values of the branch current in different intervals are determined and analyzed. The derived probability model is checked for its validity and correctness as well. The model is found to be useful for probabilistic analysis of the circuit.

Keywords: voltage probability distribution; RL circuit; probabilistic circuit analysis; inductance random variable; electric voltage probability

1. Introduction

Some constructions of the electric circuits are commonly used in different types of applications [1–6]. For example, an electric circuit comprising only resistors and a capacitor, called an RC circuit for short, is used in a wide variety of applications. Similarly, an electric circuit which only has resistors and an inductor is called an RL circuit and has multiple types of applications in a diverse range of electrical devices and equipment [7–9]. The applications of RC and RL circuits can be broadly categorized in two domains, i.e., time- and frequency-domain applications [10–14]. In typical time-domain applications, an RL circuit may be employed for the control of the timing of an event by managing the time it takes to energize or de-energize the inductor. An RL circuit may serve as an integrator or as a differentiator. It may also be used for surge suppression in an electrical network. In a frequency domain application, an RL circuit may act as a high- or low-pass filter. It is to be noted that RC circuits may also be employed for the same applications where RL circuits are used. However, in this article, our focus is on the latter, as we investigate the probability model of an exponentially decaying transient response of an RL circuit.

When used in a timing application, the time constant of the RL circuit is pivotal for provision of the time control. The time constant of an RL circuit is the inductance divided by the equivalent resistance of the circuit seen across the inductor terminals. The larger the time constant, the longer it takes to energize or de-energize the inductor, and vice versa. In frequency domain and filtering applications, the RL circuit may be used to accept or reject a certain band of frequencies. Depending upon the band of frequencies it allows or rejects, the filtering circuit may be termed as a high-pass or a low-pass filter [15–18].

A circuit for the generation of lightning impulse voltage (LIV) was investigated in [19]. The transient insulation performance of high-voltage equipment was evaluated using an LIV test. Marx's circuit, which is an RC circuit, was used for the generation of the LIV. The Glaninger's circuit is a modified form of Marx's circuit and uses an additional resistor and an inductor. The Glaninger's circuit allows testing of lower inductive value loads. The work in [19] extends Glaninger's circuit so that the inductance load can range from 400 µH to 4 mH. The work in [20] used a technique based on artificial neural network for the identification of suitable parameters for an LIV generation circuit for low inductance loads. In the conventional technique, the circuit parameters for the Glaninger's circuit were determined using a method proposed by Feser. In this approach, the circuit parameters need further adjustment so that obtained waveform is compliant with the standard requirement. This adjustment in the parameters is based on trial and error. However, using the method proposed in [20], the parameters are identified using an artificial neural network based algorithm. The work in [21] proposes a mathematical model for the commutation failure in ultra-high-voltage direct current transmission systems. The commutation failure results in a transient causing the voltage amplitude of the sending grid to first decrease and then increase. The proposed mathematical model can be used for the analysis of the transient reactive power of a doubly fed induction-generator-based wind power generation system. A simple series RL circuit was modeled using multifactor uncertain differential equation in [22]. The external and internal noise in the system were considered in the proposed model. The solution of the uncertain differential equation was derived; and the inverse uncertainty distributions, supremum and time integral of the solution were determined.

Electric circuits, including RL and RC circuits, can be investigated using a number of analysis techniques in both time and frequency domains. These analysis techniques rely on the basic principles. These principles and techniques can be applied to different types of circuits used in a diverse range of applications [23]. In addition to these fundamental techniques, there are a number of theorems which are available for circuit analysis. These theorems provide the basis for important techniques for electric circuit analysis. New theorems and techniques are also being proposed [24,25].

The aforementioned analysis techniques have only limited use if the exact value of the characteristic parameter of a circuit element is not available and it is only known to be within a range of values. This may happen to a circuit component, for example, when it develops a fault or when it is operated under unusually harsh environmental conditions, such as very high temperatures or exposure to nuclear radiation. Consequently, the characteristic parameter of the circuit element may change to a new unknown value. In these instances, probability theory alongside conventional circuit analysis techniques may be put to use for the investigation of different circuit parameters. Probability theory has been effectively used for the analysis and provision of solutions to various problems in multiple disciplines in science and engineering [26–32]. For example, it is extensively used in communication systems and signal processing applications [33,34]. The work in [35] used saddle point approximation for the estimation of hazard rate function for a linear combination of Poisson random variables. The probability distribution of the sum of two independent Poisson random variables is also Poisson. However, the probability distribution of a rescaled Poisson random variable may not be Poisson. Therefore, the distribution of a linear combination of independent Poisson random variables may not always be known. In such a situation, saddle point approximation provides helpful information about the distribution with good accuracy.

In the current work, the probability methods are exploited for the analysis of exponentially decaying transient response of an RL circuit. The inductance of a faultless inductor is a known nominal value provided by the manufacturer. However, if the inductor develops a fault, then it may no longer operate at its nominal value. The inductor may develop a fault due to a variety of factors, such as erosion of insulation material of the magnetic wire, degradation of the magnetic wire or the magnetic core, high saturation current and continuous operation at high temperature. In our work, we assumed that the inductor does not operate at its nominal value and instead has a new unknown value due to a fault. However, the inductance of the inductor was known to be within a certain continuous interval. Hence, the exact value of the inductance was not available, and we only had partial knowledge of the inductance value—the interval within which it operates. It should be further noted that we wanted to predict the circuit response under failure conditions before a fault happens. Therefore, we modeled the fault by treating the inductance as a continuous uniform random variable. The transient voltage was then considered as a derived random variable which is a function of the inductance random variable. Using the probability methods, we derived a probability model of the exponentially decaying transient voltage of the RL circuit in terms of the cumulative distribution function (CDF) and the probability density function (PDF). The derived probability model was checked for validity and correctness. In addition to the transient voltage, the probability distribution of a branch current was also obtained. Usage of the models was demonstrated with the help of examples. The probabilistic circuit analysis yields valuable results when only partial information about a circuit element is available.

Probability theory is an important tool in machine learning and artificial intelligence [36–38]. In artificial and machine learning applications, the aim is to design an intelligent machine which can perform a desired task after learning from the environment and the data. While performing a task, there may be many possible outcomes. Therefore, the machine learning model works on the basis of prediction, approximation and estimation using the data. Probability theory plays an important role in performing these important steps [39]. Likewise, the probability models developed in our work can be used for the analysis and prediction of the circuit behavior under component failure conditions. Specifically, these models can be employed for the prediction of the RL circuit's transient response under the inductor failure conditions, as is also demonstrated in this work. Therefore, these models can be utilized in the development of machine learning algorithms, thereby paving way for additional applications of these models. To the best of our knowledge, no significant work has previously been done in the probabilistic modeling of RL circuit transient response. The symbols used in this article are listed in Table 1.

Table 1. Symbols and notation.

Symbol	Description
a	Minimum value of L
b	Maximum value of L
$\mathbf{E}[X]$	Expected value of X
$F_X(x)$	CDF of random variable X
$f_X(x)$	PDF of random variable X
H	Henry
I_o	Current random variable
$i_L(0)$	Inductor current at $t = 0$
$i_L(0^-)$	Inductor current just before $t = 0$
$i_L(0^+)$	Inductor current just after $t = 0$
k_1	First constant in circuit response
k_2	Second constant in circuit response
L	Inductance random variable
l	Arbitrary value of L
mA	Milli ampere

Table 1. *Cont.*

Symbol	Description
n	Constant multiplier of τ
$P[X \leq x]$	Probability of the event $X \leq x$
R	Resistance
R_T	Thevenin equivalent resistance
$\mathbb{R}$	Set of real numbers
t	Time
τ	Time constant
u	Substitution variable
V	Volt
V_o	Voltage random variable
v_o	Arbitrary value of random variable V_o
$v_o(t)$	Instantaneous voltage
$v_o(0)$	Voltage at $t = 0$
$v_o(\infty)$	Voltage at $t = \infty$
V_x	Voltage at node x

2. RL Circuit Response

To best demonstrate our probabilistic analysis of the exponentially decaying transient response of an RL circuit, we consider the example RL circuit shown in Figure 1. All the elements in the circuit are considered to be ideal. The values of the characteristic parameters of the circuit elements are known and are labeled. However, the inductance of the inductor L1 is shown as L henries (H), as it is known only to fall within a certain continuous interval, and the exact value of the inductance is not known due to a fault. All values of the inductance in the continuous interval are equally probable. Moreover, the random value of inductance, once assigned, does not vary during the transient response. It is to be noted that the value of a working component may follow a normal distribution due to manufacturing tolerance. However, under failure conditions, the component value may follow a uniform distribution rather than a normal distribution. Switch S1 is closed, and the circuit is in a steady state. The switch is opened at $t = 0$, so that a transient occurs. After the transient is over, the circuit reaches a new steady-state condition. In this section, we perform preliminary work, and derive an expression for the RL circuit response in terms of the voltage $v_o(t)$ after switch S1 is opened. We subsequently use this response analysis for the derivation of the probability distribution of the transient response in Section 3.
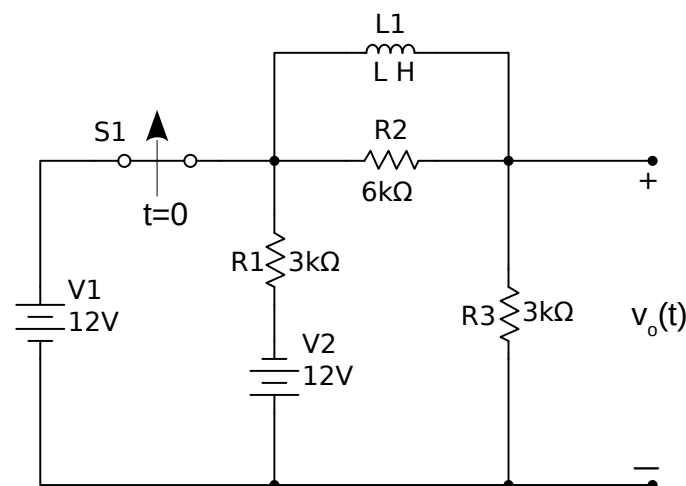

Figure 1. We investigate the response of the RL circuit after switch S1 is opened at $t = 0$. The exact value of the inductance of inductor L1 is not available and is known only to fall within a continuous interval.

In general, the voltage response of the RL circuit, shown in Figure 1 is given by

$$v_o(t) = k_1 + k_2 e^{-\frac{t}{\tau}}, \tag{1}$$

where k_1, k_2 and τ are constants, and $\tau > 0$. Moreover,

$$k_1 = v_o(\infty), \tag{2}$$

$$k_2 = v_o(0) - v_o(\infty), \tag{3}$$

$$\tau = \frac{L}{R_T}, \tag{4}$$

where $v_o(0)$ represents the initial value of the voltage v_o at $t = 0$; $v_o(\infty)$ is the voltage at $t = \infty$ under the steady-state condition; and R_T is the Thevenin equivalent resistance seen by inductor L1 after the switch is opened.

In the remainder of this section, we determine the circuit voltage response using a step-by-step analysis. In the first step, we find the initial current $i_L(0)$ through the inductor before the opening of switch S1. Next, the initial value of voltage $v_o(0)$ is determined in the second step. Then, in the third step, we find the voltage $v_o(\infty)$ under the new steady-state condition which is achieved after the transient is over. In the fourth step, the time constant τ is found by first determining the Thevenin equivalent resistance across the inductor terminals. In the last and fifth steps, the values of the different constants are determined and substituted into Equation (1) to arrive at the circuit response in terms of voltage $v_o(t)$.

2.1. Initial Current through the Inductor

Before the opening of switch S1 at $t = 0$, the circuit has attained a steady-state condition. The inductor acts as a short circuit, and a current $i_L(0^-)$ flows through it under this condition, as shown in Figure 2. The voltage and current of an inductor are related by $v = L\frac{di}{dt}$. For the current to be differentiable, it must be a continuous function. Hence, as switch S1 is opened at $t = 0$, the current through the inductor does not change instantaneously. This implies that

$$i_L(0) = i_L(0^+) = i_L(0^-). \tag{5}$$

Therefore, determination of the inductor current at $t < 0$ helps us find the initial condition of the circuit at $t = 0$. As the inductor is a short circuit at $t = 0$, there is no current through resistor R2. In addition, nodes $V_{x1}(0^-)$ and $V_{x2}(0^-)$ are at the same voltage due to the short circuit between them. It can be readily observed that

$$V_{x2}(0^-) = V_{x1}(0^-) = 12\,\text{V}. \tag{6}$$

As there is no current through R2 due to the inductor across it acting as a short circuit, it can also be observed that the current $i_L(0^-)$ through the inductor is the same as the current through the resistor R3. Therefore,

$$i_L(0^-) = \frac{12}{3k} = 4\,\text{mA}. \tag{7}$$

From Equation (5), we can write

$$i_L(0) = i_L(0^+) = i_L(0^-) = 4\,\text{mA}. \tag{8}$$

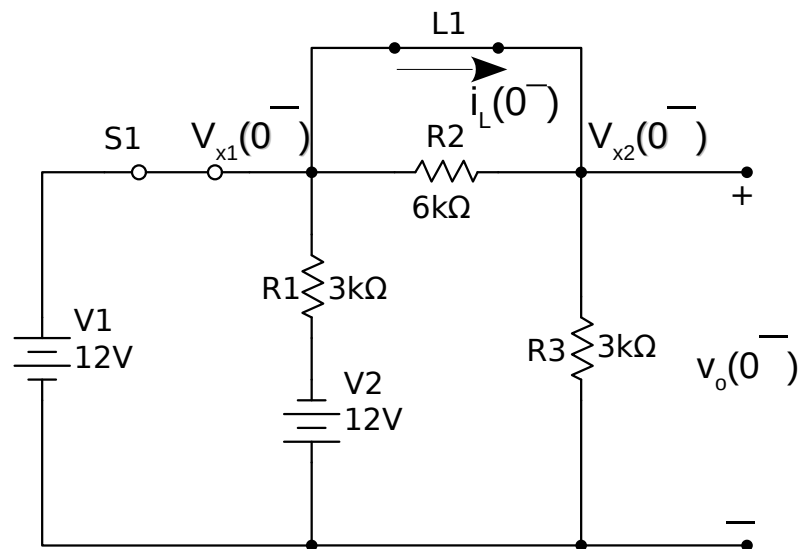This gives us the initial current through the inductor at $t = 0$.

Figure 2. Switch S1 has been closed for a long time, and the circuit has attained a steady state. The inductor acts as a short circuit, and the current through the inductor is $i_L(0^-)$.

2.2. Initial Voltage v_o at $t = 0^+$

As switch S1 is opened, the current through the inductor, i_L, does not change instantaneously between $t = 0^-$ and $t = 0^+$. Therefore, at $t = 0^+$, it can be considered as a 4 mA current source, as is shown in Figure 3. Moreover, the voltage source V1 is now no longer part of the circuit, as switch S1 is now open. To determine the voltage $v_o(0^+)$, let us consider nodes $V_{x1}(0^+)$ and $V_{x2}(0^+)$. From node $V_{x1}(0^+)$, we obtain the following:

$$\frac{V_{x1}(0^+) + 12}{3k} + \frac{V_{x1}(0^+) - V_{x2}(0^+)}{6k} + 4 = 0. \tag{9}$$

Simplification yields the following:

$$3V_{x1}(0^+) - V_{x2}(0^+) = -48. \tag{10}$$

Similarly, from node $V_{x2}(0^+)$, we have

$$\frac{V_{x2}(0^+) - V_{x1}(0^+)}{6k} + \frac{V_{x2}(0^+)}{3k} - 4 = 0. \tag{11}$$

Simplifying this, we get the following:

$$-V_{x1}(0^+) + 3V_{x2}(0^+) = 24. \tag{12}$$

When Equations (10) and (12) are solved simultaneously, we obtain

$$V_{x2}(0^+) = 3 \, V. \tag{13}$$

It can be readily observed from Figure 3 that

$$v_o(0^+) = V_{x2}(0^+) = 3 \, \text{V}. \tag{14}$$

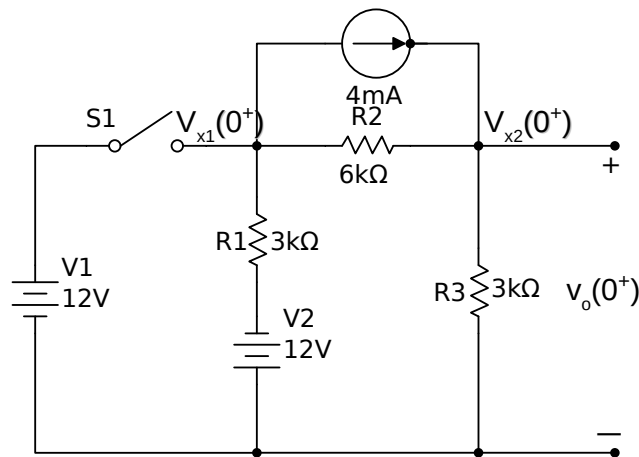This gives us the initial value of the response voltage v_o.

Figure 3. Circuit condition at $t = 0^+$ immediately after the switch $S1$ is opened. The inductor is replaced by a current source with a current equal to the initial current through the inductor.

2.3. Steady State Voltage v_o at $t = \infty$

Let us now consider the circuit under the new steady state at $t = \infty$ after a long time, equivalent to 5τ or higher, has elapsed after the opening of the switch. Under the steady-state conditions, the inductor acts as a short circuit, as is shown in Figure 4. Consequently, there is no current through resistor R2. Furthermore, it can also be observed that

$$V_{x1}(\infty) = V_{x2}(\infty). \tag{15}$$

Therefore, we obtain the following from the node

$$\frac{V_{x2}(\infty) + 12}{3k} + \frac{V_{x2}(\infty)}{3k} = 0. \tag{16}$$

Simplification gives us the following.

$$V_{x2}(\infty) = -6\,\text{V}. \tag{17}$$

As can be observed from Figure 4, $v_o(\infty) = V_{x2}(\infty)$. Therefore, the voltage v_o under the steady-state conditions is given by

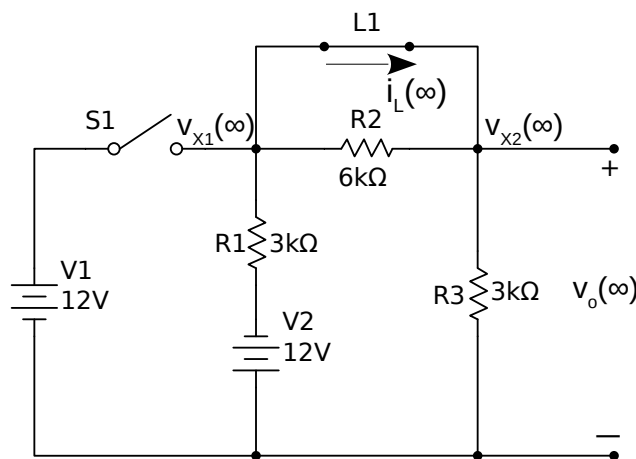$$v_o(\infty) = V_{x2}(\infty) = -6\,\text{V}. \tag{18}$$

Figure 4. Circuit at $t = \infty$ under the new steady-state condition when sufficient time has elapsed after switch S1 is opened. The inductor acts as short circuit, and a steady state current flows through it.

2.4. Time Constant

The circuit time constant can be determined from Equation (4). However, we first need to find the Thevenin equivalent resistance across the inductor terminals under the new steady-state condition at $t = \infty$. The independent source V2 is turned off to find the Thevenin equivalent resistance so that we obtain the circuit shown in Figure 5. It is observed that the Thevenin resistance across the inductor terminals is given by,

$$R_T = (R1 + R3)||R2, \tag{19}$$

$$R_T = 3\,k\Omega. \tag{20}$$

Therefore, we get the time constant as follows.

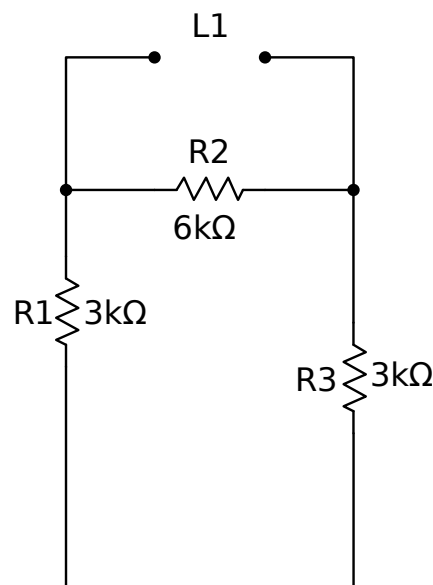$$\tau = \frac{L}{3k} \text{ seconds.} \tag{21}$$

Figure 5. The circuit to calculate the Thevenin equivalent resistance across the inductor terminals at $t > 0$. The voltage source V2 has been turned off.

2.5. Circuit Voltage Response

To determine the circuit response from Equation (1), we need to first determine constants k_1 and k_2. From Equations (2) and (18), we obtain

$$k_1 = -6. \tag{22}$$

Similarly, from Equations (3), (14) and (18), we have

$$k_2 = 3 - (-6) = 9. \tag{23}$$

By substituting Equations (21)–(23) into Equation (1), we obtain

$$v_o(t) = -6 + 9e^{-\frac{3000t}{L}} \text{ V.} \tag{24}$$

From the response in Equation (24), it can be observed that $v_o = 3$ V at $t = 0$, and $v_o = -6$ V at $t = \infty$. This is the result we already obtained in Equations (14) and (18). According to this result, the voltage v_o decreases during the transient. Therefore, the transient response in terms of the voltage v_o is an exponential decay. It can be noted that

both the initial value of the response at $t = 0$ and the final value of the response at $t = \infty$ are independent of the value of the inductance L. However, the time constant is a function of the inductance and determines how quickly the response decays and reaches the steady state. The response is plotted in Figure 6 for a convenient value of $L = \frac{1}{2}$ H. This result was confirmed by simulating the RL circuit using the same value of inductance, i.e., $L = \frac{1}{2}$ H. The simulation result is plotted in Figure 7. It can be observed that the simulation result validates the theoretical response obtained earlier.
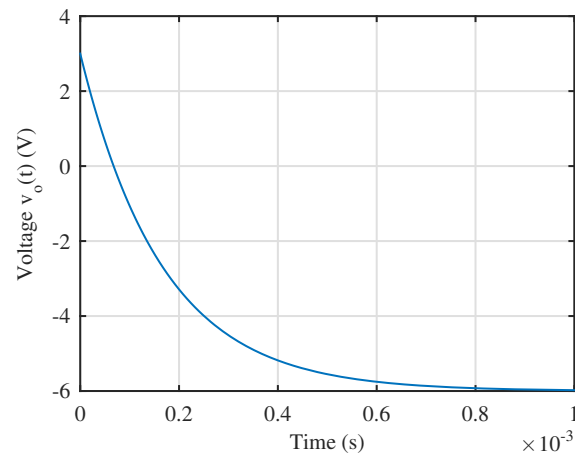

Figure 6. Transient response of the RL circuit plotted for $L = \frac{1}{2}$ H. At $t = 0$ and $v_o = 3$ V, and at $t = \infty$ and $v_o = -6$ V. The voltage $v_o(t)$ decays exponentially from $t = 0$ to $t = \infty$.
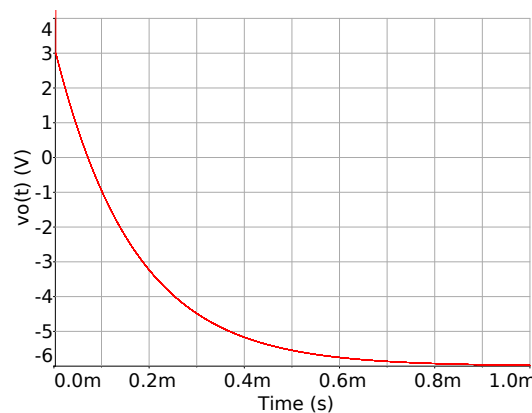

Figure 7. Simulation result of the transient response of the RL circuit using $L = \frac{1}{2}$ H.

3. Probability Distribution

In this section, we derive the probability distribution of the exponentially decaying transient response of the RL circuit. As already stated, the inductance of the inductor is known only to fall within a continuous interval, and the exact value of the inductance is not available. Therefore, we use probability methods for further investigation of the response. The inductance is treated as a random variable. Hence, the circuit response which is a function of the inductance is also a random variable. Using a probabilistic analysis, we derive the probability distribution of the exponentially decaying transient response of the RL circuit in terms of cumulative distribution function (CDF) and probability density function (PDF).

In our subsequent discussions, we denote a random variable using an upper case letter, and any of the values that it can have is represented by the corresponding lower case letter. For example, x is any one of the numerical values that a random variable X can have.

We can consider the inductance L to be a continuous, uniform, (a, b) random variable if inductance L is known to fall in the range of values a and b, such that $b > a > 0$ and $a, b \in \mathbb{R}$. Therefore, the probability density function (PDF) of L can be written as follows.

$$f_L(l) = \begin{cases} \frac{1}{b-a} & a \leq l < b, \\ 0 & \text{otherwise.} \end{cases} \tag{25}$$

The cumulative distribution function (CDF) $F_L(l)$ of L can then be written as follows.

$$F_L(l) = \begin{cases} 0 & l \leq a, \\ \frac{l-a}{b-a} & a < l \leq b, \\ 1 & l > b. \end{cases} \tag{26}$$

For the time duration $0 < t \leq 5\tau$, the circuit is in the transient state. Let us consider a time, such that

$$t = \frac{n\tau}{L}, \tag{27}$$

where $n \in \mathbb{R}$ is to be chosen such that

$$0 < t \leq 5\tau,$$
$$0 < \frac{n\tau}{L} \leq 5\tau,$$
$$0 < n \leq 5L.$$

As L is a uniform(a, b) random variable such that $a < l \leq b$, the following holds during the transient state:

$$0 < n \leq 5a. \tag{28}$$

Now, using Equation (21) in Equation (27), we obtain

$$t = \frac{n\tau}{L} = \frac{n}{3000}. \tag{29}$$

By substituting Equation (29) in Equation (24), we obtain the following for the random variable V_o:

$$V_o = -6 + 9e^{-\frac{n}{L}}. \tag{30}$$

This gives the derived random variable V_o as a function of the continuous uniform random variable L. From Equation (30), we have the following:

$$L = \frac{-n}{\ln\left[\frac{1}{9}\left(V_o + 6\right)\right]}. \tag{31}$$

It is to be noted that $V_o + 6 > 0$, i.e., $V_o > -6$, if Equation (31) is to be valid. Moreover, L is a continuous, uniform, (a, b) random variable such that $b > a > 0$, and hence, $L > 0$. Therefore, the denominator term in Equation (31) should satisfy the following.

$$\ln\left[\frac{1}{9}\left(V_o + 6\right)\right] < 0, \tag{32}$$

so that we obtain $L > 0$.

3.1. Probability Model of V_o

The probability model of the random variable V_o, which is a function of L, can be obtained by deriving its cumulative distribution function (CDF) $F_{V_o}(v_o)$. By definition, the CDF $F_{V_o}(v_o)$ is given by

$$F_{V_o}(v_o) = P[V_o \leq v_o].$$

(33)

We can evaluate the expression $V_o \leq v_o$ using Equation (30), as follows.

$$-6 + 9e^{-\frac{n}{L}} \leq v_o,$$

$$\frac{n}{L} \geq -\ln\left[\frac{1}{9}(v_o + 6)\right].$$

(34)

It can be concluded from Equations (31) and (32) that $-\ln\left[\frac{1}{9}(v_o + 6)\right] > 0$ in Equation (34). Therefore, by taking the reciprocal of Equation (34) and then multiplying by n, we get the following.

$$L \leq \frac{-n}{\ln\left[\frac{1}{9}(v_o + 6)\right]}.$$

(35)

We can now derive the CDF from Equations (33) and (35), as follows.

$$F_{V_o}(v_o) = P\left[L \leq \frac{-n}{\ln\left[\frac{1}{9}(v_o + 6)\right]}\right],$$

(36)

As $F_L(l) = P[L \leq l]$, Equation (36) yields the following.

$$F_{V_o}(v_o) = F_L\left(\frac{-n}{\ln\left[\frac{1}{9}(v_o + 6)\right]}\right).$$

(37)

Therefore, using Equation (26), we have the following.

$$\frac{l-a}{b-a} = \frac{-n}{(b-a)\left[\ln\left[\frac{1}{9}(v_o + 6)\right]\right]} - \frac{a}{b-a}.$$

(38)

It can be observed from Equation (26) that we should derive the expressions for the three intervals for v_o which correspond to $l \leq a$, $a < l \leq b$ and $l > b$ for a complete specification of $F_{V_o}(v_o)$. These three intervals are determined in the following.

3.1.1. $l \leq a$

We begin with the interval corresponding to

$$l \leq a.$$

From Equation (31), we have the following.

$$\frac{-n}{\ln\left[\frac{1}{9}(v_o + 6)\right]} \leq a,$$

$$v_o \leq -6 + 9e^{-\frac{n}{a}}. \tag{39}$$

This gives us the interval for $F_{V_o}(v_o)$ corresponding to the interval $l \leq a$ for $F_L(l)$.

3.1.2. $l > b$

Similarly, the expression for the interval corresponding to the interval $l > b$ for $F_L(l)$ is obtained using (31) in the following.

$$l > b,$$

$$\frac{-n}{\ln\left[\frac{1}{9}(v_o + 6)\right]} > b,$$

$$v_o > -6 + 9e^{-\frac{n}{b}}. \tag{40}$$

3.1.3. $a < l \leq b$

Using a similar procedure, we obtain the expression for the third interval as follows.

$$a < l \leq b,$$

$$a < \frac{-n}{\ln\left[\frac{1}{9}(v_o + 6)\right]} \leq b,$$

$$-6 + 9e^{-\frac{n}{a}} < v_o \leq -6 + 9e^{-\frac{n}{b}}. \tag{41}$$

3.1.4. The CDF

The complete CDF $F_{V_o}(v_o)$ can now be obtained using Equations (38)–(41), as

$$F_{V_o}(v_o) = \begin{cases} 0 & v_o \leq -6 + 9e^{-\frac{n}{a}}, \\ \dfrac{-n}{(b-a)\left[\ln\left[\frac{1}{9}(v_o+6)\right]\right]} - \dfrac{a}{b-a} & -6 + 9e^{-\frac{n}{a}} < v_o \leq -6 + 9e^{-\frac{n}{b}}, \\ 1 & v_o > -6 + 9e^{-\frac{n}{b}}. \end{cases} \tag{42}$$

3.1.5. The PDF

By differentiating the CDF in Equation (42), we get the PDF, as

$$f_{V_o}(v_o) = \frac{\mathrm{d}}{\mathrm{d}v_o}\left[\frac{-n}{(b-a)\left[\ln\left[\frac{1}{9}(v_o + 6)\right]\right]} - \frac{a}{b-a}\right],$$

$$f_{V_o}(v_o) = \frac{n}{(b-a)(v_o + 6)\left[\ln\left[\frac{1}{9}(v_o + 6)\right]\right]^2}. \tag{43}$$

$$f_{V_o}(v_o) = \begin{cases} \dfrac{n}{(b-a)(v_o+6)\left[\ln\left[\frac{1}{9}(v_o+6)\right]\right]^2} & -6 + 9e^{-\frac{n}{a}} \leq v_o < -6 + 9e^{-\frac{n}{b}}, \\ 0 & \text{otherwise.} \end{cases} \tag{44}$$

We can use either the CDF in Equation (42) or the PDF in Equation (44) as a complete probability model of the random variable V_o, and hence, that of the exponentially decaying transient response of the RL circuit under investigation.

3.2. Validity of the Model

The validity of the derived probability model is confirmed if the following is found to hold for Equation (44):

$$\int_{-\infty}^{+\infty} f_{V_o}(v_o)dv_o = 1. \tag{45}$$

Using Equation (44) in Equation (45), we get

$$\int_{-\infty}^{+\infty} f_{V_o}(v_o)dv_o = \int_{-6+9e^{-\frac{n}{a}}}^{-6+9e^{-\frac{n}{b}}} \frac{n}{(b-a)(v_o+6)\left[\ln\left[\frac{1}{9}(v_o+6)\right]\right]^2}dv_o. \tag{46}$$

We can solve this using the substitution method. Therefore, let

$$u = \ln\left[\frac{1}{9}(v_o+6)\right]. \tag{47}$$

Hence,

$$\frac{\mathrm{d}u}{\mathrm{d}v_o} = \frac{1}{v_o+6}, \tag{48}$$

$$\mathrm{d}v_o = (v_o+6)\mathrm{d}u. \tag{49}$$

We now derive the limits for u with respect to Equation (46). These are determined to be

$$u = -\frac{n}{a}. \tag{50}$$

$$u = -\frac{n}{b}. \tag{51}$$

Substituting Equations (47) and (49) in Equation (46), and using the limits in Equations (50) and (51), we get

$$\int_{-\infty}^{+\infty} f_{V_o}(v_o)dv_o = \frac{n}{(b-a)}\int_{-\frac{n}{a}}^{-\frac{n}{b}}\frac{\mathrm{d}u}{u^2}, \tag{52}$$

$$\int_{-\infty}^{+\infty} f_{V_o}(v_o)dv_o = \frac{n}{(b-a)}\left|-\frac{1}{u}\right|_{-\frac{n}{a}}^{-\frac{n}{b}} = 1. \tag{53}$$

Therefore, the derived probability model is a valid model, as Equation (45) is found to hold for Equation (44).

3.3. Expected Value

The expected value of V_o, which is the first moment around origin, is given by

$$\mathbf{E}[V_o] = \int\limits_{-\infty}^{+\infty} v_o f_{V_o}(v_o)\mathrm{d}v_o, \tag{54}$$

$$\mathbf{E}[V_o] = \int\limits_{-6+9e^{-\frac{n}{a}}}^{-6+9e^{-\frac{n}{b}}} \frac{n v_o}{(b-a)(v_o+6)\left[\ln\left[\frac{1}{9}(v_o+6)\right]\right]^2}\mathrm{d}v_o. \tag{55}$$

This is evaluated to be

$$\mathbf{E}[V_o] = \frac{n}{b-a}\left|\frac{-v_o}{\ln\left(\frac{v_o+6}{9}\right)} + 9\mathrm{li}\left(\frac{v_o+6}{9}\right)\right|_{-6+9e^{-\frac{n}{a}}}^{-6+9e^{-\frac{n}{b}}}, \tag{56}$$

$$\mathbf{E}[V_o] = \frac{n}{b-a}\left[\frac{-b(6-9e^{-\frac{n}{b}})}{n} + \frac{a(6-9e^{-\frac{n}{a}})}{n}\right] + \frac{9n}{b-a}\left[\mathrm{Ei}(-\frac{n}{b}) - \mathrm{Ei}(-\frac{n}{a})\right]. \tag{57}$$

4. Application of the Probability Model

In this section, we discuss some applications of the probability model. Derivation of the probability models of other circuit parameters is also described and discussed.

4.1. Examples

To illustrate the use of the probability distribution, let us consider an example. Let $a = \frac{1}{4}$ H and $b = \frac{3}{4}$ H so that the expected value of the uniformly distributed, continuous random variable L is $\mathbf{E}[L] = \frac{1}{2}$ H. By using these values of a and b in Equations (25) and (26), we obtain the following PDF and CDF of L for this specific case.

$$f_L(l) = \begin{cases} 2 & \frac{1}{4} \leq l < \frac{3}{4}, \\ 0 & \text{otherwise,} \end{cases} \tag{58}$$

$$F_L(l) = \begin{cases} 0 & l \leq \frac{1}{4}, \\ 2l - \frac{1}{2} & \frac{1}{4} < l \leq \frac{3}{4}, \\ 1 & l > \frac{3}{4}. \end{cases} \tag{59}$$

In conformance with Equation (28), we assume $n = a = \frac{1}{4}$ H. Therefore, using Equation (29), we get $t = \frac{1}{12000}$ s. This time instant lies within the transient state because $\frac{1}{4} < l \leq \frac{3}{4}$, and it is noted from Equation (21) that $t = \frac{1}{12000} \leq \tau$. Using $a = \frac{1}{4}$, $b = \frac{3}{4}$ and $n = a = \frac{1}{4}$ in Equation (42), we have the CDF as follows:

$$F_{V_o}(v_o) = \begin{cases} 0 & v_o \leq -2.69, \\ \frac{-1}{2\ln\left[\frac{1}{9}(v_o+6)\right]} - \frac{1}{2} & -2.69 < v_o \leq 0.449, \\ 1 & v_o > 0.449. \end{cases} \tag{60}$$

In a similar manner, the PDF for our example is obtained from Equation (44), as

$$f_{V_o}(v_o) = \begin{cases} \dfrac{1}{2(v_o+6)\left[\ln\left[\frac{1}{9}(v_o+6)\right]\right]^2} & -2.69 \leq v_o < 0.449, \\ 0 & \text{otherwise.} \end{cases} \tag{61}$$

The probability model for the specific case when $L \sim \text{uniform}(\frac{1}{4}, \frac{3}{4})$ is given by the CDF in Equation (60) and the PDF in Equation (61). We plot the CDF and PDF for this specific case in Figures 8 and 9, respectively.
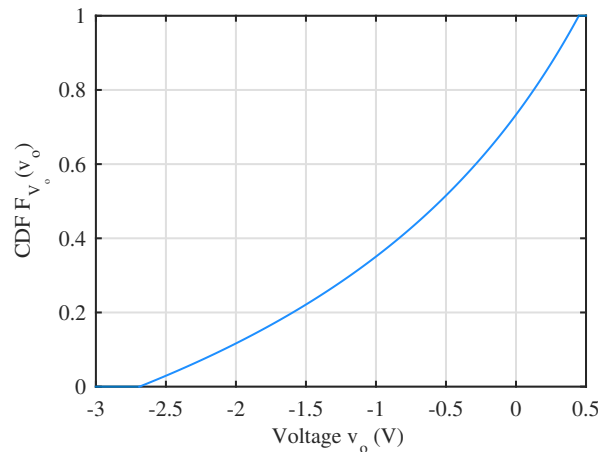

Figure 8. The cumulative distribution function (CDF) $F_{V_o}(v_o)$ when L is a uniform, (a, b), continuous random variable, such that $a = \frac{1}{4}$ H, $b = \frac{3}{4}$ H.
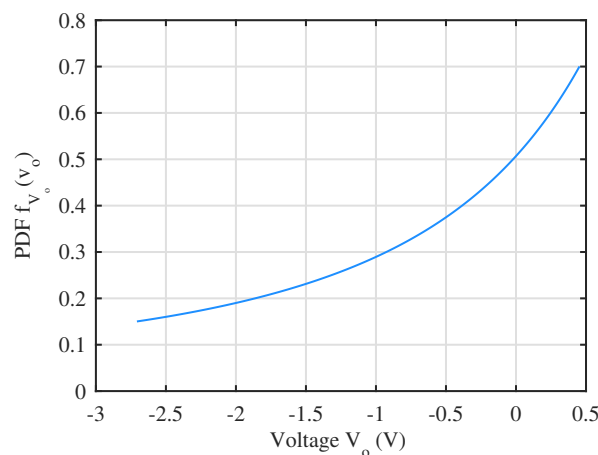

Figure 9. The probability density function (PDF) $f_{V_o}(v_o)$ when L is a uniform, (a, b), continuous random variable, such that $a = \frac{1}{4}$ H, $b = \frac{3}{4}$ H.

We can calculate probabilities for different values of v_o using the CDF and the PDF. For further illustration, let us compute the probability $P[V_o \leq 0]$. We can note from Equations (60) and (61) that $F_{V_o}(v_o) = 0$ and $f_{v_o}(v_o) = 0$ for $v_o < -2.69$. Therefore,

$$P[V_o \leq 0] = P[-2.69 < V_o \leq 0]. \tag{62}$$

We can evaluate Equation (62) using Equation (61) as follows:

$$P[V_o \leq 0] = \int_{-2.69}^{0} f_{V_o}(v_o)\mathrm{d}v_o, \tag{63}$$

$$P[V_o \leq 0] = \int_{-2.69}^{0} \frac{dv_o}{2(v_o + 6)\left[\ln\left[\frac{1}{9}(v_o + 6)\right]\right]^2}, \tag{64}$$

This can be evaluated using the substitution in Equation (47). Using Equation (47), we find the lower limit $u = -1$ when $v_o = -2.69$, and the upper limit $u = -0.4055$, when $v_o = 0$. By substituting Equations (47) and (49) in Equation (64), and using the obtained limits, we get

$$P[V_o \leq 0] = \frac{1}{2} \int_{-1}^{-0.4055} \frac{du}{u^2}, \tag{65}$$

$$P[V_o \leq 0] = \frac{1}{2}\left| -\frac{1}{u} \right|_{-1}^{-0.4055} = 0.733. \tag{66}$$

This same result can also be obtained from Equation (60) more easily, as follows:

$$P[V_o \leq 0] = F_{V_o}(0) = 0.733. \tag{67}$$

We can state that the probability that v_o is between -2.69 V and 0 V is 73.3%. This also implies that

$$P[V_o > 0] = P[0 < V_o \leq 0.449], \tag{68}$$

$$P[V_o > 0] = 1 - P[V_o \leq 0] = 0.267. \tag{69}$$

The expected value for this specific example can also be calculated using Equation (61), as below.

$$\mathbf{E}[V_o] = \int_{-2.69}^{0.449} \frac{v_o}{2(v_o + 6)\left[\ln\left[\frac{1}{9}(v_o + 6)\right]\right]^2} dv_o, \tag{70}$$

$$\mathbf{E}[V_o] = -0.725 \, \text{V}. \tag{71}$$

This expected value can also be calculated by substituting the values of a, b and n in Equation (57).

All these probability values, and the expected value, for the example under consideration, are calculated for the time instant $t = \frac{1}{12}$ ms. By selecting an appropriate value of n, the probability values and the expected value for any other time instant can be calculated in a similar manner. The probability model can be exploited for the prediction of the circuit response and for the development of machine learning algorithms [38,39].

4.2. Other Circuit Parameters

We can derive the probability distribution of any other circuit parameter, such as a voltage or a current, using the same procedure that we used for the derivation of the probability model of the voltage V_0. The voltage or the current for which the probability model is to be derived is usually first expressed as a function of L. The probability distribution in terms of CDF and PDF can then be derived by following the method we have already illustrated. It is also possible that a circuit parameter is expressed as a function of V_o, whose probability model has already been obtained. In such a scenario, it is possible that the probability model of the parameter can be derived from the already

derived model for V_o. For further illustration, let us consider the current through the resistor R3 in the downward direction. Let us represent this current by I_o. It is given by

$$I_o = \frac{V_o}{3k}. \tag{72}$$

If we choose mA as the unit for I_o, then this can be simply expressed as

$$I_o = \frac{V_o}{3} \text{ mA}. \tag{73}$$

We can observe that I_o is a derived random variable which is a function of V_o as its constant multiple. Therefore, the relationship between the desired CDF $F_{I_o}(i_o)$ and the CDF $F_{V_o}(V_o)$, which is already available, can be established in the following manner:

$$F_{I_o}(i_o) = P[I_o \leq i_o], \tag{74}$$

By substituting that into Equation (73), we obtain

$$F_{I_o}(i_o) = P\left[\frac{V_o}{3} \leq i_o\right], \tag{75}$$

$$F_{I_o}(i_o) = P\left[V_o \leq 3i_o\right], \tag{76}$$

Therefore,

$$F_{I_o}(i_o) = F_{V_o}(3i_o). \tag{77}$$

We obtained the CDF $F_{I_o}(i_o)$ from Equations (42) and (77) as follows:

$$F_{I_o}(i_o) = \begin{cases} 0 & i_o \leq -2 + 3e^{-\frac{n}{a}}, \\ \dfrac{-n}{(b-a)\left[\ln\left[\frac{1}{3}\left(i_o+2\right)\right]\right]} - \dfrac{a}{b-a} & -2 + 3e^{-\frac{n}{a}} < i_o \leq -2 + 3e^{-\frac{n}{b}}, \\ 1 & i_o > -2 + 3e^{-\frac{n}{b}}. \end{cases} \tag{78}$$

The relationship between the PDFs $f_{I_o}(i_o)$ and $f_{V_o}(v_o)$ is obtained by differentiating Equation (77), as follows:

$$f_{I_o}(i_o) = \frac{dF_{I_o}}{di_o}, \tag{79}$$

$$f_{I_o}(i_o) = \frac{d}{di_o}F_{V_o}(3i_o), \tag{80}$$

$$f_{I_o}(i_o) = 3f_{V_o}(3i_o). \tag{81}$$

We can now obtain the PDF $f_{I_o}(i_o)$ using Equations (44) and (81) as follows:

$$f_{I_o}(i_o) = \begin{cases} \dfrac{n}{(b-a)(i_o+2)\left[\ln\left[\frac{1}{3}(i_o+2)\right]\right]^2} & -2 + 3e^{-\frac{n}{a}} \leq i_o < -2 + 3e^{-\frac{n}{b}}, \\ 0 & \text{otherwise.} \end{cases} \tag{82}$$

It is to be noted that the unit of the current I_o in the CDF given by Equation (78) and the PDF given by Equation (82) is mA.

Using Equation (82), the expected value of I_o is given by

$$\mathbf{E}[I_o] = \int_{-2+3e^{-\frac{n}{a}}}^{-2+3e^{-\frac{n}{b}}} \frac{ni_o}{(b-a)(i_o+2)\left[\ln\left[\frac{1}{3}(i_o+2)\right]\right]^2}\, di_o. \tag{83}$$

$$\mathbf{E}[I_o] = \frac{n}{b-a}\left[\frac{-b(2-3e^{-\frac{n}{b}})}{n} + \frac{a(2-3e^{-\frac{n}{a}})}{n}\right] + \frac{3n}{b-a}\left[\text{Ei}(-\frac{n}{b}) - \text{Ei}(-\frac{n}{a})\right]. \tag{84}$$

4.3. Example for I_o

The use of the probability distribution of I_o given by Equations (78) and (82) is now explained with the help of an example. To this end, let us consider the probability model of L given by Equations (58) and (59). Therefore, $a = \frac{1}{4}$ H, $b = \frac{3}{4}$ H and $n = a = \frac{1}{4}$ H. We obtained the CDF for our example by using these values in Equation (78) as follows.

$$F_{I_o}(i_o) = \begin{cases} 0 & i_o \leq -0.8964, \\ \frac{-1}{2\ln\left[\frac{1}{3}(i_o+2)\right]} - \frac{1}{2} & -0.8964 < i_o \leq 0.1496, \\ 1 & i_o > 0.1496. \end{cases} \tag{85}$$

In a similar manner, we obtained the PDF for our example from Equation (82) as below.

$$f_{I_o}(i_o) = \begin{cases} \frac{1}{2(i_o+2)\left[\ln\left[\frac{1}{3}(i_o+2)\right]\right]^2} & -0.8964 \leq i_o < 0.1496, \\ 0 & \text{otherwise.} \end{cases} \tag{86}$$

The CDF in Equation (85) and the PDF in Equation (86) can be used for the probabilistic analysis of I_o in the same manner that we used for the analysis of V_o using the CDF in Equation (42) and the PDF in Equation (44). Let us compute the probability, say, $P[I_o \leq 0.05]$, as an example. We can calculate this using Equations (85) or (86). Let us use Equation (85) for the sake of convenience.

$$P[I_o \leq 0.05] = F_{I_o}(0.05) = 0.8131. \tag{87}$$

Stated in words, this says that the probability that the current i_o is between -0.8964 and 0.05 mA at $t = \frac{10^{-3}}{12}$ s when L~uniform$(\frac{1}{4}, \frac{3}{4})$ is 81.31%. To give another example, let us calculate the probabilities for two equal but different intervals—say, $P[-0.8 < I_o \leq -0.4]$ and $P[-0.4 < I_o \leq 0]$. The probabilities are given as

$$P[-0.8 < I_o \leq -0.4] = F_{I_o}(-0.4) - F_{I_o}(-0.8) = 0.2497, \tag{88}$$

$$P[-0.4 < I_o \leq 0] = F_{I_o}(0) - F_{I_o}(-0.4) = 0.4378. \tag{89}$$

Therefore, the probability that the current i_o is between -0.4 and 0 mA is 43.78%, which is higher than the probability 24.97% that it is between -0.8 and -0.4 mA.

The expected value of I_o for this specific example can be either determined by substituting the values of constants in Equation (84) or by definition using Equation (86). The expected value, in this case, is determined to be

$$\mathbf{E}[I_o] = -0.2417\,\text{mA}. \tag{90}$$

The expected value falls in the interval $[-4, 0]$ mA for which the probability is given by Equation (89) and is found to be higher than that for the $[-0.8, -0.4]$ mA interval.

5. Conclusions

We have exploited probability methods for the analysis of the exponentially decaying transient response of an RL circuit with partial knowledge of the inductance value in this article. The inductance is known to be within a certain continuous interval. However, the exact value is not known. This situation may arise as a result of a fault—for example, when the circuit is deployed in harsh conditions or any other factors. We treated the inductance as a continuous uniform random variable and derived an expression for the exponentially decaying transient response. The probability model of the required transient voltage was then obtained by treating it as a derived random variable which is a function of the inductance. The probability model of a branch current was also derived. Usage of the models was demonstrated with the help of examples. The developed probability distribution can be exploited for the development of machine learning algorithms also. Therefore, probabilistic circuit analysis is useful for the investigation of an RL circuit transient response in uncertain conditions when only partial information about the inductance is available. In future, the work may be extended to circuits involving failure of more than one circuit component.

Author Contributions: Conceptualization, M.F.-i.-A.; methodology, R.A. and S.R.H.; validation, M.F.-i.-A., Z.H.K. and S.R.H.; investigation, Z.H.K.; resources, R.A.; writing—original draft preparation, M.F.-i.-A.; writing—review and editing, S.R.H., Z.H.K. and R.A.; visualization, Z.H.K.; supervision, M.F.-i.-A.; project administration, S.R.H. and R.A. All authors have read and agreed to the published version of the manuscript.

Institutional Review Board Statement: Not applicable.

Informed Consent Statement: Not applicable.

Data Availability Statement: Not applicable.

Conflicts of Interest: The authors declare no conflict of interest.

References

1. Gu, Y.; Feng, X.; Chi, R.; Wu, J.; Chen, Y. A Digital Bang-Bang Clock and Data Recovery Circuit Combined with ADC-Based Wireline Receiver. *Electronics* **2022**, *11*, 3489. [CrossRef]
2. Mu, Y.; Hou, N.; Wang, C.; Zhao, Y.; Chen, K.; Chi, Y. An Optoelectronic Detector with High Precision for Compact Grating Encoder Application. *Electronics* **2022**, *11*, 3486. [CrossRef]
3. Ketata, I.; Ouerghemmi, S.; Fakhfakh, A.; Derbel, F. Design and Implementation of Low Noise Amplifier Operating at 868 MHz for Duty Cycled Wake-Up Receiver Front-End. *Electronics* **2022**, *11*, 3235. [CrossRef]
4. Jin, X.Z.; Che, W.W.; Wu, Z.G.; Wang, H. Analog Control Circuit Designs for a Class of Continuous-Time Adaptive Fault-Tolerant Control Systems. *IEEE Trans. Cybern.* **2020**, *52*, 4209–4220. [CrossRef]
5. Sun, J.; Han, G.; Zeng, Z.; Wang, Y. Memristor-Based Neural Network Circuit of Full-Function Pavlov Associative Memory with Time Delay and Variable Learning Rate. *IEEE Trans. Cybern.* **2020**, *50*, 2935–2945. [CrossRef]
6. Liu, L.; Liu, Y.J.; Li, D.; Tong, S.; Wang, Z. Barrier Lyapunov Function-Based Adaptive Fuzzy FTC for Switched Systems and Its Applications to Resistance–Inductance–Capacitance Circuit System. *IEEE Trans. Cybern.* **2020**, *50*, 3491–3502. [CrossRef]
7. Wan, F.; Li, N.; Ravelo, B.; Ji, Q.; Li, B.; Ge, J. The Design Method of the Active Negative Group Delay Circuits Based on a Microwave Amplifier and an RL-Series Network. *IEEE Access* **2018**, *6*, 33849–33858. [CrossRef]
8. Xu, D.; Zhang, W.; Shi, P.; Jiang, B. Model-Free Cooperative Adaptive Sliding-Mode-Constrained-Control for Multiple Linear Induction Traction Systems. *IEEE Trans. Cybern.* **2020**, *50*, 4076–4086. [CrossRef]
9. Lin, Y.S.; Wang, Y.E. Design and Analysis of a 94-GHz CMOS Down-Conversion Mixer With CCPT-RL-Based IF Load. *IEEE Trans. Circuits Syst. I Regul. Pap.* **2019**, *66*, 3148–3161. [CrossRef]
10. Kondo, J.; Tanzawa, T. Pre-Emphasis Pulse Design for Reducing Bit-Line Access Time in NAND Flash Memory. *Electronics* **2022**, *11*, 1926. [CrossRef]
11. Gagliardi, F.; Manfredini, G.; Ria, A.; Piotto, M.; Bruschi, P. Low-Phase-Noise CMOS Relaxation Oscillators for On-Chip Timing of IoT Sensing Platforms. *Electronics* **2022**, *11*, 1794. [CrossRef]
12. Ahmed, O.; Khan, Y.; Butt, M.A.; Kazanskiy, N.L.; Khonina, S.N. Performance Comparison of Silicon- and Gallium-Nitride-Based MOSFETs for a Power-Efficient, DC-to-DC Flyback Converter. *Electronics* **2022**, *11*, 1222. [CrossRef]

13. Sobhan Bhuiyan, M.A.; Hossain, M.R.; Minhad, K.N.; Haque, F.; Hemel, M.S.K.; Md Dawi, O.; Ibne Reaz, M.B.; Ooi, K.J.A. CMOS Low-Dropout Voltage Regulator Design Trends: An Overview. *Electronics* **2022**, *11*, 193. [CrossRef]

14. Ko, J.; Lee, M. A 1.8 V 18.13 MHz Inverter-Based On-Chip RC Oscillator with Flicker Noise Suppression Using Logic Transition Voltage Feedback. *Electronics* **2019**, *8*, 1353. [CrossRef]

15. Wang, Y.; Yu, M.; Ma, K. A Compact Low-Pass Filter Using Dielectric-Filled Capacitor on SISL Platform. *IEEE Microw. Wirel. Components Lett.* **2021**, *31*, 21–24. [CrossRef]

16. Wang, S.F.; Chen, H.P.; Ku, Y.; Zhong, M.X. Analytical Synthesis of High-Pass, Band-Pass and Low-Pass Biquadratic Filters and its Quadrature Oscillator Application Using Current-Feedback Operational Amplifiers. *IEEE Access* **2021**, *9*, 13330–13343. [CrossRef]

17. Yang, M.; Wang, H.; Yang, T.; Hu, B.; Li, H.; Zhou, Y.; Li, T. Design of wide Stopband for Waveguide low-pass Filter Based on Circuit and Field Combined Analysis. *IEEE Microw. Wirel. Components Lett.* **2021**, *31*, 1199–1202. [CrossRef]

18. Şengül, M.; Çakmak, G.; Özdemir, R. Phase Shifting Properties of High-Pass and Low-Pass Mixed-Element Two-Ports. *IEEE Trans. Circuits Syst. II Express Briefs* **2021**, *68*, 1208–1212. [CrossRef]

19. Yutthagowith, P.; Kitcharoen, P.; Kunakorn, A. Systematic Design and Circuit Analysis of Lightning Impulse Voltage Generation on Low-Inductance Loads. *Energies* **2021**, *14*, 8010. [CrossRef]

20. Tuethong, P.; Kitwattana, K.; Yutthagowith, P.; Kunakorn, A. An Algorithm for Circuit Parameter Identification in Lightning Impulse Voltage Generation for Low-Inductance Loads. *Energies* **2020**, *13*, 3913. [CrossRef]

21. Nian, H.; Jin, X. Modeling and Analysis of Transient Reactive Power Characteristics of DFIG Considering Crowbar Circuit under Ultra HVDC Commutation Failure. *Energies* **2021**, *14*, 2743. [CrossRef]

22. Liu, Y.; Zhou, L. Modeling RL Electrical Circuit by Multifactor Uncertain Differential Equation. *Symmetry* **2021**, *13*, 2103. [CrossRef]

23. Xie, L.; Huang, J.; Tan, E.; He, F.; Liu, Z. The Stability Criterion and Stability Analysis of Three-Phase Grid-Connected Rectifier System Based on Gerschgorin Circle Theorem. *Electronics* **2022**, *11*, 3270. [CrossRef]

24. Reverter, F.; Gasulla, M. A Novel General-Purpose Theorem for the Analysis of Linear Circuits. *IEEE Trans. Circuits Syst. II Express Briefs* **2021**, *68*, 63–66. [CrossRef]

25. Barbi, I. A Theorem on Power Superposition in Resistive Networks. *IEEE Trans. Circuits Syst. II Express Briefs* **2021**, *68*, 2362–2363. [CrossRef]

26. Li, Z.; Tang, L.; Liu, J. A Memetic Algorithm Based on Probability Learning for Solving the Multidimensional Knapsack Problem. *IEEE Trans. Cybern.* **2020**, *52*, 2284–2299. [CrossRef]

27. Song, S.; Cheng, M.; He, J.; Zhou, X.; Matsumoto, T. Outage Probability of One-Source-With-One- Helper Sensor Systems in Block Rayleigh Fading Multiple Access Channels. *IEEE Sensors J.* **2021**, *21*, 2140–2148. [CrossRef]

28. Nguyen Duc, H.; Nguyen Hong, N. Optimal Reserve and Energy Scheduling for a Virtual Power Plant Considering Reserve Activation Probability. *Appl. Sci.* **2021**, *11*, 9717. [CrossRef]

29. Li, L.; Huang, Z.; Zhou, J. A Two-Stage Maximum a Posterior Probability Method for Blind Identification of LDPC Codes. *IEEE Signal Process. Lett.* **2021**, *28*, 111–115. [CrossRef]

30. Tan, Y.; Liu, Q.; Liu, J.; Xie, X.; Fei, S. Observer-Based Security Control for Interconnected Semi-Markovian Jump Systems With Unknown Transition Probabilities. *IEEE Trans. Cybern.* **2021**, *52*, 9013–9025. [CrossRef]

31. Hareli, S.; Nave, O.; Gol'dshtein, V. The Evolutions in Time of Probability Density Functions of Polydispersed Fuel Spray—The Continuous Mathematical Model. *Appl. Sci.* **2021**, *11*, 9739. [CrossRef]

32. Sun, L.; Deng, Z. A Fast and Robust Rotation Search and Point Cloud Registration Method for 2D Stitching and 3D Object Localization. *Appl. Sci.* **2021**, *11*, 9775. [CrossRef]

33. Okoth, M.A.; Shang, R.; Jiao, L.; Arshad, J.; Rehman, A.U.; Hamam, H. A Large Scale Evolutionary Algorithm Based on Determinantal Point Processes for Large Scale Multi-Objective Optimization Problems. *Electronics* **2022**, *11*, 3317. [CrossRef]

34. Odeyemi, K.O.; Owolawi, P.A.; Olakanmi, O.O. On Secrecy Performance of a Dual-Hop UAV-Assisted Relaying Network with Randomly Distributed Non-Colluding Eavesdroppers: A Stochastic Geometry Approach. *Electronics* **2022**, *11*, 3302. [CrossRef]

35. Al Mutairi, A. Advanced Approach for Estimating Failure Rate Using Saddlepoint Approximation. *Symmetry* **2021**, *13*, 2041. [CrossRef]

36. Ghahramani, Z. Probabilistic machine learning and artificial intelligence. *Nature* **2015**, *521*, 452–459. [CrossRef]

37. Abdul Majid, A. Forecasting Monthly Wind Energy Using an Alternative Machine Training Method with Curve Fitting and Temporal Error Extraction Algorithm. *Energies* **2022**, *15*, 8596. [CrossRef]

38. Ranftl, S. A Connection between Probability, Physics and Neural Networks. *Phys. Sci. Forum* **2022**, *5*, 11. [CrossRef]

39. Anthony, M. Probability Theory in Machine Learning. In *Encyclopedia of the Sciences of Learning*; Seel, N.M., Ed.; Springer: Boston, MA, USA, 2012; pp. 2677–2680. [CrossRef]